High spatial resolution studies of phase transitions within organic aperiodic crystals

Céline Mariette, Laurent Guérin, Philippe Rabiller, Christophe Odin, Mariana Verezhak, Alexei Bosak, Philippe Bourges, Claude Ecolivet, Bertrand Toudic

High spatial resolution studies of phase transitions within organic aperiodic crystals

Céline Mariette,[1,*] Laurent Guérin,[1,†] Philippe Rabillier,[1] Christophe Odin,[1] Mariana Verezhak,[1,2] Alexei Bosak,[3] Philippe Bourges,[4] Claude Ecolivet,[1] and Bertrand Toudic[1,‡]

[1] *Univ. Rennes, CNRS, IPR (Institut de Physique de Rennes) - UMR 6251, F-35000 Rennes, France*

[2] *Paul Scherrer Institut, Forschungsstrasse 111, 5232 Villigen, Switzerland*

[3] *European Synchrotron Radiation Facility, BP 220, 38043 Grenoble Cedex, France*

[4] *Université Paris-Saclay, CNRS, CEA, Laboratoire Léon Brillouin, 91191, Gif-sur-Yvette, France*

(Dated: February 28, 2020)

Abstract

The understanding of the symmetry breakings within crystals that are aperiodic by construction is actually very limited. Quasicrystals and incommensurate composite crystals may potentially allow such studies. We focus in this article on the phase transitions of the aperiodic *n*-nonadecane/urea which recovers a translational symmetry within a four dimensional space at room temperature. High resolution neutron and synchrotron studies are reported as function of the temperature on this organic crystal which presents an exceptional mosaicity. They reveal the richness of such approach showing the appearance of very long wavelength supplementary intermodulations. This work generalizes the Landau theory to incommensurate composite crystals.

I. INTRODUCTION

Phase transitions and critical phenomena in matter are fundamental fields of research since a century. Huge progresses were made in formalism with the Landau mean field theory and later on with the renormalization group theory [1, 2]. In parallel, the field extends to crystals which are not periodic in the three dimensional space. Simultaneously, a huge breakthrough came from the experimental side. Synchrotron radiations offer high flux with low divergence, which allowed to develop highly selective techniques leading to exceptional resolution in reciprocal space. However, in order to take benefit of these ultra-high spatial resolutions, some conditions are requested for the studied crystal itself. There, it appears that organic crystals may present a so perfect mosaicity that it is not even measurable on the best high resolution spectrometers. This opens the possibility to study symmetry breakings properties never explored up to now around phase transitions such as critical phenomena or within aperiodic crystals. The new definition of the crystal by the International Union of Crystallography includes the materials that present long range order without translational symmetry. The periodicity of such crystals is recovered in higher dimensional spaces, called crystallographic superspaces [3–6] that are characterized by more than three independent basis vectors. The quasiperiodic crystals are usually divided in three families: the incommensurately modulated ones, the incommensurate composite crystals and the quasicrystals.

* celine.mariette@univ-rennes1.fr

† laurent.guerin@univ-rennes1.fr

‡ bertrand.toudic@univ-rennes1.fr

Much work has been dedicated to these three families focussing on their structures, their dynamics and other physical properties [7–12]. Concerning structural instabilities in these materials, the incommensurate modulated crystals have been extensively and definitively successfully explained [6]. Indeed, the incommensurate phase is the result of a phase transition from a 3 dimensional periodic space to a (3+1) or a (3+2) dimensions where their periodicity is recovered. The superspace group describing these incommensurate phases is directly related to the periodic space group of the high symmetry phase [6, 7, 13, 14]. Quasicrystals and incommensurate composite crystals do not present any high symmetry periodic phase which makes their studies of course much more difficult. Phase transitions within quasicrystals have not really been analysed in the literature. More works have been dedicated to incommensurate composite crystals [7, 15–19]. A peculiar case corresponds to host/guest intergrowth nanotubular structures, which have a sole incommensurate direction called here c. There, periodicity is recovered in a four dimensional space and a four-dimensional superspace description gives the positions of the complete set of Bragg peaks [3, 4, 7]: $\boldsymbol{Q_{hklm}} = h\boldsymbol{a^*} + k\boldsymbol{b^*} + l\boldsymbol{c_h^*} + m\boldsymbol{c_g^*}$ where $\boldsymbol{a^*}$, $\boldsymbol{b^*}$, $\boldsymbol{c_h^*}$ and $\boldsymbol{c_g^*}$ are the conventional reciprocal unit cell vectors, and $\boldsymbol{c_h}$ and $\boldsymbol{c_g}$ refer, respectively, to the host and the guest parameters along the aperiodic direction. Four indices are needed to describe four different types of structure Bragg peaks (h k l m): a convenient but simplistic labeling is that (h k 0 0), (h k l 0), (h k 0 m) and (h k l m) with l and m different from zero are the common, host, guest, and satellite Bragg peaks, respectively. Within this family of aperiodic intergrowth nanotubular structures, the organic guest/host n-alkane/urea compounds constitute a prototype family [7, 20–39]. In almost all of the n-alkane/urea inclusion compounds, a four dimensional hexagonal superspace group $P6_122(00\gamma)$ is reported in the literature at room temperature. The parameters for the host urea subsystem are then $a_{hex} = b_{hex} = 8.22$ $\mathring{A}$, and the pitch of the urea helix is $c_{host} = c_h = 11.02$ $\mathring{A}$ [27]. In the case of hydrogenated (linear) n-alkane/urea, an empirical experimental estimation of the guest periodicity c_g was reported by Lenné et al. [21]: c_g = [1.277 (n-1) + 3.48] $\mathring{A}$, where n is the number of carbon atoms in the alkane molecule. In most cases, the ratio of the host and guest parameter is irrational defining a misfit parameter $\gamma = (c_h/c_g) = (c_g^*/c_h^*)$. These compounds are then aperiodic by construction. They present structural phase transitions which have been studied since many years. However, in earlier studies, aperiodicity was not considered as important for the single phase transition detected at that time. Consequently, theoretical

works limited their description to the common periodic $(\boldsymbol{a}, \boldsymbol{b})$ plane where a ferroelastic shear occurs [22–24, 26, 40]. Somehow, this corresponds to the simplistic description of a two dimensional problem and not a three and a fortiori not a four dimensional one. Due to the lack of resolution, they wrongly observed the appearance of superstructure Bragg peaks within the basal $(\boldsymbol{a}^*, \boldsymbol{b}^*)$ plane and thus they concluded for an antiferrodistorsion of the host urea sublattice and an herringbone ordering of the guest alkane molecules [24–26]. Considering the aperiodic feature of the crystal, we reported experimental results and theoretical interpretations within crystallographic superspaces in total contradiction with this established interpretation. Much of our work was dedicated to n-nonadecane/urea [31, 33, 35]. The reference [31] concerns experimental data performed at atmospheric pressure within the so-called phases II and III of n-nonadecane/urea, whereas the reference [33] reports experimental data under pressure at 0.5GPa in a different phase, called phase IV. In this article, the superspace groups of these different phases are given. According to adiabatic calorimetric measurements, several phase transitions were reported in these crystals, the transition temperatures presenting isotopic effects [41]. These transition temperatures are announced at $T_{c1} = 158.8\ K$ and $T_{c2} = 147\ K$ for the fully hydrogenated $C_{19}H_{40}/CO(NH_2)_2$ compound and at $T_{c1}^D = 149.4\ K$ and $T_{c2}^D = 127.8\ K$ for the fully deuterated $C_{19}D_{40}/CO(ND_2)_2$. Very recently, some authors questioned this work [42, 43]. They argue in favor of a single ferroelastic phase transition described in the $(\boldsymbol{a}, \boldsymbol{b})$ plane [26, 44]. We strongly contested this work [45, 46]. We present here high resolution synchrotron data which prove the originality of the phase transitions when described by taking into account their aperiodic feature by construction.

II. SYMMETRY BREAKING INDUCED DOMAINS

The symmetry breaking was extensively studied many years ago considering the symmetry induced domains. At that time a single phase transition was considered in n-alkane/urea compounds at a transition temperature T_c, that we will call T_{c1} in the present article. The phase transition was observed from hexagonal to orthorhombic with the appearance of a splitting of the basal Bragg peaks. They correspond to differently oriented domains. These domains result from the loss of the six fold screw axis along the channel direction. The two sets of three domains (1, 2, and 3) further rotate by a small angle of the order of ± 1

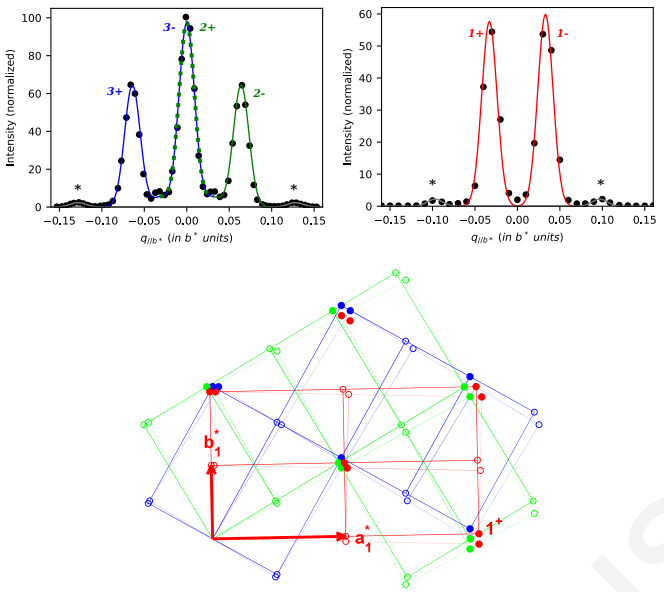

FIG. 1. Thermal neutron diffraction measured at the Laboratoire Léon Brillouin on a triple axis spectrometer (1T) of the $(\boldsymbol{a}^*, \boldsymbol{b}^*)$ plane of n-nonadecane /urea in the ferroelastic phase. The measurement was performed at T = 100 K on a fully deuterated crystal. These two scans correspond to two measurements of the maxima of the intensity associated to the low symmetry induced domains. They are measured for h=4 and k=0, as defined in the schematic figure below considering the domain 1. Top left, measurement along b* in h=3.86, top right, same measurement in h=4. Schematic representation of the diffraction image, identifying the six different domains is shown in the bottom. Red, blue and green refer to 3 types of symmetry induced domains generated by the lost of the 3 fold symmetry element going from the hexagonal to the orthorhombic phase (domains 1, 2 , 3, respectively). A supplementary splitting is observed with a small tilt angle apart the mean value [24], defining six perfectly separate types of domains respectively called 1+, 1-, 2+, 2-, 3+, 3-. Further studies presented in the article are performed in a single type of domains, called conventionally 1+. The asterisk mark other small supplementary mis-oriented domains [40].

degree as shown by Forst et al. [24] and that is explained in terms of energetic arrangements. Weber [40] observed the existence of supplementary smaller domains with a double rotational angle. Our neutron scattering experiments were performed in the Laboratoire Léon Brillouin at the Orphée reactor (Saclay, France). The diffraction data were collected on the triple axis spectrometer 1T installed on a thermal neutron source. The incident wave vector was

$k_i = 2.662\ \mathring{A}^{-1}$. A standard setup was used with no collimations and a Pyrolytic Graphite filter was installed on k_f to remove the higher order harmonics. The retained scattering plane was the periodic $(\boldsymbol{a}^*, \boldsymbol{b}^*)$ one. With this study of fully deuterated *n*-nonadecane/urea on a much bigger crystal than used for X-ray, we confirm the above experimental result with also the same proportion of these domains (1, 2 and 3). The supplementary small domains are pointed by an asterisk in the figures 1 (top left and right). In the following part of this article, we will focus on the diffraction signature of *n*-nonadeacane/urea along the direction perpendicular to the $(\boldsymbol{a}^*, \boldsymbol{b}^*)$ plane using cold neutrons scattering and X-ray synchrotron diffraction. In both cases, the spatial resolution in the reciprocal space allows the selection of one single domain, the so-called domain 1+ in the figures 1 (top left and bottom).

III. THE SEQUENCE OF PHASES

Several articles have already been dedicated to the measurements along the reciprocal channel axis of *n*-nonadecane/urea [29, 31, 33, 35, 47]. The first papers proved the aperiodic feature of *n*-nonadecane/urea showing the existence of the structure Bragg peaks appearing at combinatory positions, that is Bragg peaks with the indices (h, k, l, m) with l and m simultaneously different from zero [29, 47]. This was a proof of the reciprocal intermodulation of the host (urea) and the guest (*n*-nonadecane) sublattices. The other papers [31, 33, 35] focused on the phase transitions that appear in this crystal as function of the temperature. In order to drastically reduce the incoherent neutron scattering of the hydrogen atoms, fully deuterated crystals have actually to be used for the neutron scattering studies. Figure 2 reports the diffraction profile measured using neutron scattering on the fully deuterated crystal along the direction $\boldsymbol{c}^*$, perpendicular to the $(\boldsymbol{a}^*, \boldsymbol{b}^*)$ plane. Neutron scattering experiments were performed in the Laboratoire Léon Brillouin at the Orphée reactor (Saclay, France). The diffraction data were collected on the triple axis spectrometer 4F installed on a cold neutron source. The incident wave vector was $k_i = 2.662\ \mathring{A}^{-1}$. The energy resolution being of the order of 100 μeV, it means that phonons are not integrated within the presented elastic measurements. The retained scattering plane was the aperiodic $(3\boldsymbol{a}^* + 2\boldsymbol{b}^*, \boldsymbol{c}^*)$ plane, according to the domain 1+ orthorhombic notation. The scan ranges from l = -1.5 to 0.5, that is around the host reciprocal positions (l = -1) and around the common Bragg peak (l = 0). In the case of the fully deuterated *n*-nonadecane/urea, a first ordered phase, called

phase II, spreads between $T_{c1}^D = 149.4\ K$ and $T_{c2}^D = 127.8\ K$. The systematic absence of the common and host superstructure Bragg peaks (defined by h+k odd in the orthorhombic low symmetry domain 1+) in this phase has been discussed extensively in previous articles [33]. A supplementary intermodulation of the crystal appears within this phase II. It is associated to the appearance of strong Bragg peaks, very slightly away from the common reciprocal position, as shown in the figure 2 (top). A similar feature appears around the host reciprocal position. These Bragg peaks are located at $\pm\delta c_h^*$ apart from these two reciprocal positions. According to this measurement, the wavelength of the supplementary modulation was of the order of $c_h/\delta = 120\ \mathring{A}$, δ being found equal to 0.091 ± 0.005. A lower ordered phase, called III, appears below $T_{c2}^D = 127.8\ K$ in the fully deuterated n-nonadecane/urea. There, superstructure Bragg peaks are present in the common l = 0 position, as shown at T = 100 K in the figure 2 (top). The so-called satellites at $\pm\delta c_h^*$ are still present at this temperature showing the persistence of the associated supplementary intermodulation. The lowest temperature measurement by neutron scattering in the phase II at T = 128 K reveals supplementary satellites very close to the common and the host superstructure position, but clearly still out of these positions as shown in the figure 2 (bottom).

In order to analyze these diffraction peaks, an even better spatial resolution is required. Therefore, high spatial resolution studies have been performed using the inelastic backscattering spectrometer ID28 at the synchrotron ESRF at Grenoble, France. The optical layout is based on the triple-axis principle. The energy resolution is obtained by a monochromator Si(12,12,12), in backscattering geometry. The scattered photons are energy analyzed by a perfect spherical silicon crystal analyzer, operated in Rowland geometry. The X-rays diffracted from the analyzer crystal are recorded by solid-state detectors (low-noise silicon detectors), that present a very low background. The incident photon wavelength was then $\lambda = 0.5227\ \mathring{A}$ ($E \simeq 23.7\ keV$) and the energy resolution was $1.5\ meV$ [39] in a wide part of the reciprocal space up to $10\mathring{A}^{-1}$. This energy resolution means that only very low frequency acoustic phonons are integrated within the presented elastic measurements. Such thermal diffuse scattering can thus be ignored. The spatial resolution is at least of the order of 0.7 μm, as discussed later on. The organic nature of the n-nonadecane/urea $C_{19}H_{40}/CO(NH_2)_2$ sample requires a large single crystal, in this case: $0.5 \times 0.5 \times 1cm^3$, in order to maximize the scattered intensity. The size of the crystals used for neutrons and inelastic X-ray scattering are similar and their growing are done according the same process.

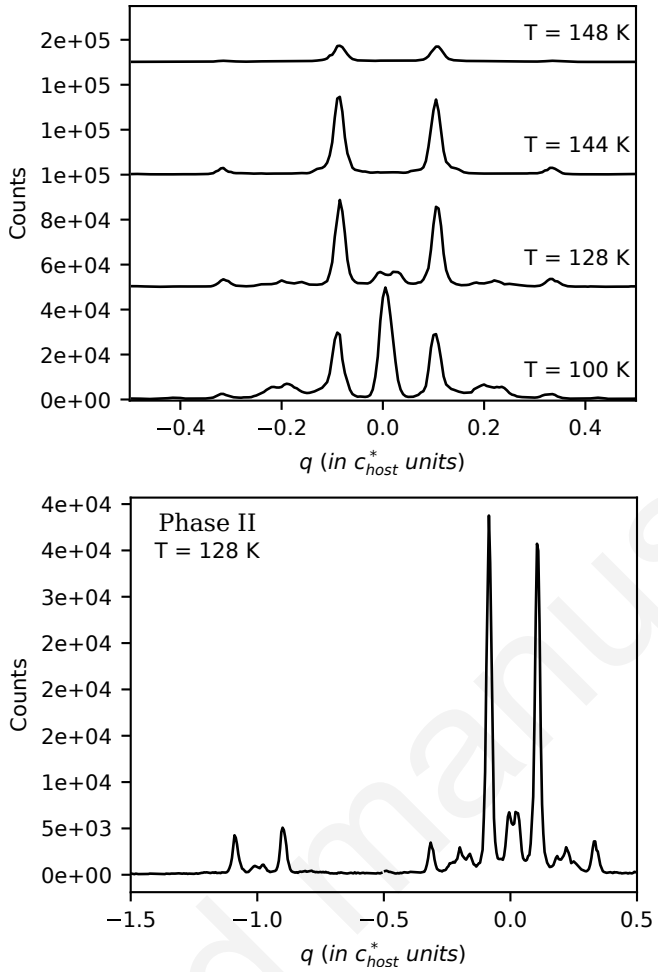

FIG. 2. Cold neutron diffraction measured at the Laboratoire Léon Brillouin on a triple axis spectrometer (4F). The sample was a fully deuterated n-nonadecane/urea single crystal (T_{c1} = 149.4 K, T_{c2} = 127.8 K). Top : Limited q-range scan around common reciprocal position (3 2 0 0), along $\boldsymbol{c^*}$ from -0.5 to +0.5 in urea c^*_h reciprocal units. Temperature decreasing from top to bottom, respectively T = 148 K, 144 K, 128 K and 100 K. Bottom : At T = 128 K, full range scan along the same reciprocal $\boldsymbol{c^*}$ line around both urea (3 2 -1 0) and common (3 2 0 0) reciprocal position from -1.5 to +0.5 in urea c^*_h reciprocal units.

This instrument is used as a triple axis spectrometer allowing the required scan within the reciprocal space. These studies were performed on a fully hydrogenated $C_{19}H_{40}/CO(NH_2)_2$ single crystal. Like in the neutron study, the diffraction measurements were performed on a single selected domain equivalent to the so called "domain 1+". The use of highly selective X-ray backscattering monochromator drastically decreases the incoming X-ray flux, thus ensuring that no substantial damage is created in the samples during these data acquisitions.

A. Critical pretransitional phenomena within the high symmetry phase $P6_122(00\gamma)$

Measurements were performed in the high symmetry phase along the aperiodic direction c*, around the reciprocal (3 0 3 0) position. They reveal the existence of diffuse scattering with maxima around $\pm\delta c_h^*$ (see profiles shown in figure 3). Quite long correlation lengths ξ are extracted from the fit of the data at T = 165 K by the usual $S(q,T) = k_B T/(q^2 + \xi^{-2})$ function: $\xi = 700\,\mathring{A}$ at T = 175 K and $\xi = 850\,\mathring{A}$ at T = 165 K. The feature of this critical diffuse scattering has been extensively discussed in [35]. The grey curves in figure 3 corresponds to the diffraction profile of the Bragg peaks in the ordered phase II (T = 158 K). According to the width of these peaks, the length of the long range order within this crystal is of the order of $0.70\,\mu m$. The spatial resolution by neutron scattering is certainly defined by the spectrometer itself, whereas the X-ray backscattering spectrometer permits to measure some Bragg broadening. The related typical peak width (1 mrad FWHM) is superior to the beam divergence and is likely to be determined by the mosaicity of crystal.

Such long correlation lengths within the high symmetry phase reveal the very low energy cost to generate spatial pretransitional fluctuations of the order parameter along the aperiodic direction [35]. In that direction, a specific excitation has been reported, the so-called sliding mode [48]. Its existence was revealed via a coupling with the longitudinal acoustic phonon propagating along that direction. It corresponds in a theoretical description to the zero energy anti-translational longitudinal mode of the host and guest subsystems. The softening of such an excitation may induce a supplementary intermodulation analog to a soft phonon mode which generates incommensurate static modulation in an incommensurate modulated crystals [6]. Dynamical studies are in progress to test this hypothesis.

B. The ordered ferroelastic phase II, between T_{c1} and T_{c2} : $C222_1(00\gamma)(10\delta)$

The measurement performed by neutron scattering in the phase II at T = 128 K is shown in the figure 2 (bottom) both around the host (l = -1) and the common (l=0) reciprocal point. Whereas some complexity appears in the scan, the intensity presents a minimum at these two positions. Actually, this measure reveals the already reported Bragg peaks at $\pm 0.091\ \boldsymbol{c_h^*}$, but in addition other Bragg peaks much closer to the common and the host reciprocal positions. The figure 4 presents the measurement performed by inelastic synchrotron scattering of the

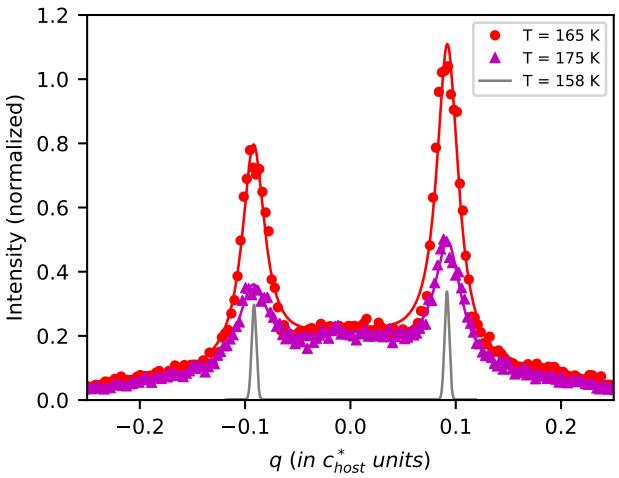

FIG. 3. Diffraction profiles measured on the inelastic X-ray backscattering spectrometer at the ESRF (ID28). Scan along the reciprocal direction $\boldsymbol{c^*}$ around (3 0 3 0) host reciprocal position, above $T_{c1} = 160\,K$ (Fully hydrogenated n-nonadecane/urea single crystal), at T = 165 K (red) and 175 K (magenta). The associated plain colored lines are the refined profiles as described in the text. The same scan is shown in phase II (T = 158 K, grey plain lines) to show the typical Bragg peak profile that defines here the momentum resolution.

fully hydrogenated single crystal in the phase II at T = 135 K. We could not measure main Bragg peaks together as it would damage the detectors, but they were aligned with the absorber, and the scans along the reciprocal direction $\boldsymbol{c^*}$ were performed within well-defined orientation matrix. For this reason, in order not to saturate the detector, the measurement could not be performed around the common reciprocal position, so only the study around the host reciprocal positions could be done. However, the neutron study shown in figure 2 (top) reveals that a similar behaviour is reported around both host and common reciprocal positions. A very complex structure is reported by X-ray synchrotron diffraction with a series of maxima as shown in the figure 4. Note that in this measurement, horizontal beam divergence was equal to $150\,\mu rad$ (FWHM), which is still an order of magnitude smaller than the splitting of satellites along c* (± 1 mrad, determined around (3 0 3 0 0) Bragg peak position). The main point is that with this high spatial resolution, the intensity is zero in the host reciprocal position. The second major feature is the new value for the misfit parameter are extracted from these data. According to the fit shown in the figure 4, this value is found equal to 0.0048 ± 0.0005 in c^*_h units. With such a so short reciprocal vector,

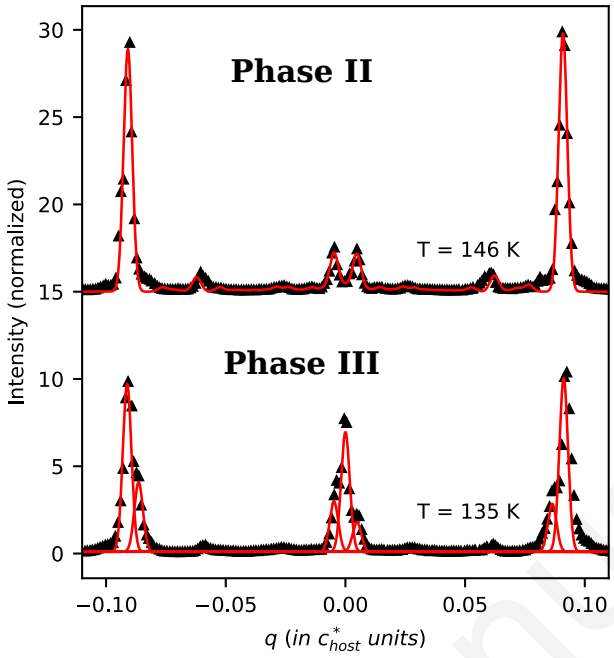

FIG. 4. Diffraction profiles measured on the inelastic X-ray backscattering spectrometer at the ESRF (ID28). Scan along the reciprocal direction $\boldsymbol{c}^*$ around (3 0 3 0) host reciprocal position in phase II, T = 146 K and phase III, T = 135 K. Measurements were performed on fully hydrogenated n-nonadecane/urea ($T_{c1} = 160\,K$, $T_{c2} = 145K$). Measured data are shown with black triangles, refined patterns in plain red lines. Here, the five dimensional notation of the Bragg peaks is used : $\boldsymbol{Q_{hklmn}}$ = h $\boldsymbol{a}^*$ + k $\boldsymbol{b}^*$ + l $\boldsymbol{c}_{\boldsymbol{h}}^*$ + m $\boldsymbol{c}_{\boldsymbol{g}}^*$ + n $\boldsymbol{c}_{\boldsymbol{m}}^*$ (see text). In the phase II, the fitted Bragg peaks fulfill the condition of presence h+k+n even, the fifth supplementary parameter being $c_m^* = (0.0048 \pm 0.0005)\ c_h^*$. In phase II, we report significant satellite Bragg peaks with n = ± 1, ± 13, ± 19. For phase III, individual contributions of the refined Bragg peaks are also displayed. Bragg peaks appear with n = 0 and n = ± 18.

values of the indices l and m higher than 100 would be needed to express the position of this satellite in the four dimensional combination (l c_h^* + m c_g^*) (within the precision of our data). So, such a description can be ruled out here. Following the previous assumption of a five dimensional superspace characterized by five indices (h, k l, m, n) we define the following vector $\boldsymbol{Q_{hklmn}} = h\boldsymbol{a}^* + k\boldsymbol{b}^* + l\boldsymbol{c}_{\boldsymbol{h}}^* + m\boldsymbol{c}_{\boldsymbol{g}}^* + n\boldsymbol{c}_{\boldsymbol{m}}^*$ where $\boldsymbol{c}_{\boldsymbol{m}}^* = \delta\boldsymbol{c}_{\boldsymbol{h}}$. In the figure 4 the satellites are indexed by only odd numbers (n=1,3,...). The strong maxima at ±0.091,

corresponds to n = 19 considering this new reciprocal periodicity. The wavelength of this intermodulation is given by $c_m = c_h/\delta$: this reciprocal position corresponds to a value of the wavelength of the supplementary incommensurate intermodulation along the channels of the order of $0.23\,\mu m$, which is extremely large. Due to the sensibility of the detector, the high resolution of this spectrometer and the exceptional mosaicity of the crystal, a so long period of the supplementary modulation can be observed by inelastic X-ray scattering.

The systematic condition of absence of the host and common superstructure h+k+n odd observed in the phase II is in favour of the five dimensional superspace number 20.2.24.2 [49]: $C222_1(00\gamma)(10\delta)$. This superspace group is a subgroup of the high symmetry superspace group $P6_122(00\gamma)$, considering a critical wavevector (1/2 1/2 0 0 1/2) within this high temperature phase. The scientific meaning of this phase group as applied to *n*-nonadecane/urea is explicitely given in [35]. The fifth parameter is associated to the appearance of a supplementary intermodulation of both host and guest sublattices along the channel direction. This intermodulation is in antiphase for adjacent channels along the diagonal of the orthorhombic phase (see figure 2 in ref. [35]). Unfortunately, it is not possible to perform a structure refinement in the low temperature phases because there are so many symmetry induced domains as shown in figure 1.

C. The ordered phase III, between T_{c2} and T_{c3}: $P2_12_12_1(00\gamma)(00\delta)$

An essential change appears in the temperature range between T = 146 K and T = 135 K as shown in the diffraction patterns in the figure 4 (bottom). We observe a new phase, called phase III, signed by the appearance of a very narrow superstructure Bragg peaks here in the host reciprocal position. This symmetry breaking is more clearly illustrated in the figure 5 with a zoom on the central part of the diffraction image around the host reciprocal position. In the neutron scattering measurements, a similar appearance of a superstructure Bragg peak at common reciprocal position is observed as the signature of the phase III (figure 2). This result confirms that the structural change around $T_{c2} = 145K$ is a real phase transition, associated to the loss of the centering within a five dimensional space. No condition of absence exist anymore for h+k+n in this phase III, where the C centering is lost, leading to a primitive unit cell in the phase III. This phase is described by a five dimensional superspace group number 19.2.18.1 [49] $P2_12_12_1(00\gamma)(00\delta)$, which is a subgroup

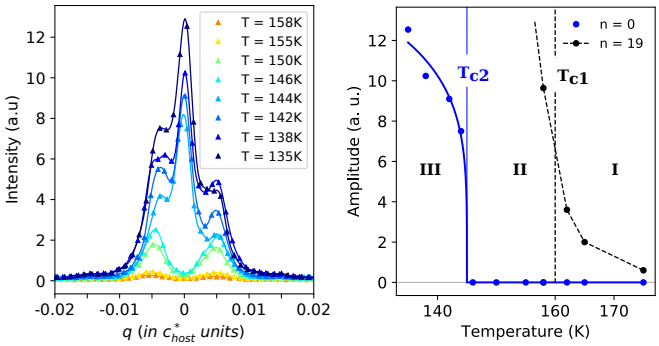

FIG. 5. Diffraction profiles measured on the inelastic X-ray backscattering spectrometer at the ESRF (ID28). Left: Zoom on the Scan along the reciprocal direction $\boldsymbol{c}^*$ around (3 0 3 0) host reciprocal position. Fully hydrogenated n-nonadecane/urea ($T_{c1} = 160K$, $T_{c2} = 145K$) in phase II and phase III. Right: Integrated intensity at satellite position (3 0 3 0 19) verifying the condition of presence h+k+n even (black) and position (3 0 3 0 0) verifying the condition h+k+n odd (blue) as a function of temperature, defining the clear sequence of three phases.

of the superspace group of the phase II. Let us mention that a supplementary phase appears below a temperature T_{c3} of the order of 60 K in the fully deuterated sample [37].

IV. CONCLUSION

Superspace crystallography is the tool to describe aperiodic crystals, recovering translational symmetry within higher dimensional space larger than three. The n-alkane/urea compounds are prototype examples of incommensurate composite crystals. Most of them are described at room temperature by a four dimensional hexagonal superspace group. From the first work [22], and during more than three decades [23–27], the aperiodic feature was not considered there explicitly and a 3D description was done when considering the phase transition. We had later shown that the phase transition requires a 5D description for the low temperature phases of n-nonadecane/urea [33]. There is a fundamental structural change when considering the previous 3D description (which is actually a bi-dimensional description) and the 5D one. In a theoretical article, Lynden-Bell [26] considered one single phase transition for all n-alkane/urea, describing the ordering in the commensurate basal plane $(\boldsymbol{a}, \boldsymbol{b})$, perpendicular to the channels. With her calculation, she found two possible structural solutions for this phase transition. One is an antiferroshearing of the host urea sublattice

with a herringbone ordering of the guest: this induces a doubling in the basal plane perpendicular to the incommensurate channel axis. At that time, due to bad spatial resolution, the superstructure Bragg peaks were indeed observed by error in the basal reciprocal space $(\boldsymbol{a}^*, \boldsymbol{b}^*)$ in h+k odd positions. So, the community agreed for a single phase transition from hexagonal $P6_122$ to orthorhombic $P2_12_12_1$ [23–27]. The second solution corresponds to an ordering of the alkane molecules all parallel and a ferroshearing of the host. This meant no Bragg peaks in the $(\boldsymbol{a}^*, \boldsymbol{b}^*)$ plane at (h+k odd), as we indeed report in the phase II. Of course, this is a quite limited representation of the structural ordering within this phase. In addition, since satellite Bragg peaks appear along the incommensurate directions out of the $(\boldsymbol{a}^*, \boldsymbol{b}^*)$ at h+k odd, we have to assume a doubling of the unit cell within the crystallographic superspace.This C-centered $C222_1(00\gamma)(10\delta)$ five dimensional superspace group for the phase II has been extensively described in previous articles [36, 38]. The present study reports in n-nonadecane/urea a wavelength for the new incommensurate intermodulation along the aperiodic direction $(0.23\mu m)$ much longer than the one previously reported doing neutron scattering studies [31, 33] due to the very high momentum resolution of the X-ray backscaterring spectrometer. This very high resolution permits also to clearly determine the temperature evolution of the order parameter signing the second symmetry breaking at T_{c2} leading to the superspace group $P2_12_12_1(00\gamma)(10\delta)$. The same very long wavelength of the supplementary modulation $(0.23\ \mu m)$ is found in this phase III according to the precision of our data. As mentioned in the introduction, recently two studies argued that there is one single phase transition in n-nonadecane/urea from $P6_122(00\gamma)$ to $P2_12_12_1(00\gamma)$ [42–44], as initially proposed. Their model considers again the critical point M within the reciprocal $(\boldsymbol{a}^*, \boldsymbol{b}^*)$ plane [44]. We have shown here that this is not correct: in phase II the critical wave vector is outside the $(\boldsymbol{a}^*, \boldsymbol{b}^*)$, in the point (1/2, 1/2, 0, 0, 1/2) of the five dimensional Brillouin zone [33, 36, 38]. It corresponds to a completely different symmetry within a Landau description of the phase transition. This work shows that incommensurate composite crystals may present complicated structural features which can be only revealed using very high momentum resolution diffractometers. The inelastic X-ray backscattering spectrometer used here fits these requirements. This generation of instruments give new opportunities to study symmetry breakings and their related critical pretransitional phenomena with new perspectives. This opens a large field of research for revisiting phase transitions in matter.

ACKNOWLEDGMENTS

We thank Tomasz Breczewski for providing the large fully hydrogenated and fully deuterated single crystals, and M. D. Hollingsworth for very fruitful discussions.

[1] K. G. Wilson, Rev. Mod. Phys. **55**, 583 (1983).

[2] L. Landau and E. Lifshitz, *Statistical Physics (Third Edition)*, third edition ed. (Butterworth-Heinemann, Oxford, 1980).

[3] P. M. de Wolff, T. Janssen, and A. Janner, Acta Crystallographica Section A **37**, 625 (1981).

[4] T. Janssen, A. Janner, A. Looijenga-Vos, and P. M. de Wolff, in *International Tables for Crystallography* (International Union of Crystallography, Chester, England, 2006) pp. 907–955.

[5] S. van Smaalen, *Incommensurate Crystallography* (Oxford University Press, 2007).

[6] R. R. Blinc and A. P. Levaniuk, *Incommensurate phases in dielectrics* (North-Holland, 1986).

[7] T. Janssen, G. Chapuis, and M. de Boissieu, *Aperiodic crystals : from modulated phases to quasicrystals : structure and properties* (2007).

[8] P. Coppens, Acta Crystallographica Section B **51**, 402 (1995).

[9] S. Van Smaalen and K. D. M. Harris, Proceedings of the Royal Society of London. Series A: Mathematical, Physical and Engineering Sciences **452**, 677 (1996).

[10] D. Shechtman, I. Blech, D. Gratias, and J. W. Cahn, Phys. Rev. Lett. **53**, 1951 (1984).

[11] D. Gratias and M. Quiquandon, Philosophical Magazine **88**, 1887 (2008).

[12] T. Janssen, Acta Crystallographica Section A **68**, 667 (2012).

[13] J. C. Tolédano and P. Tolédano, *The Landau Theory of Phase Transitions* (WORLD SCIENTIFIC, 1987).

[14] H. T. Stokes and B. J. Campbell, Acta Crystallographica Section A **73**, 4 (2017).

[15] P. A. Albouy, J. P. Pouget, and H. Strzelecka, Phys. Rev. B **35**, 173 (1987).

[16] J. M. Hastings, J. P. Pouget, G. Shirane, A. J. Heeger, N. D. Miro, and A. G. MacDiarmid, Phys. Rev. Lett. **39**, 1484 (1977).

[17] I. U. Heilmann, J. D. Axe, J. M. Hastings, G. Shirane, A. J. Heeger, and A. G. MacDiarmid, Phys. Rev. B **20**, 751 (1979).

[18] M. I. McMahon and R. J. Nelmes, Phys. Rev. Lett. **93**, 055501 (2004).

[19] E. Castillo-Martnez, A. Schnleber, S. van Smaalen, A. Arvalo-Lpez, and M. Alario-Franco, Journal of Solid State Chemistry **181**, 1840 (2008).

[20] R. C. Pemberton and N. G. Parsonage, Trans. Faraday Soc. **61**, 2112 (1965).

[21] H.-U. Lenné, H.-C. Mez, and W. Schlenk jr., Justus Liebigs Annalen der Chemie **732**, 70 (1970).

[22] Y. Chatani, H. Anraku, and Y. Taki, Molecular Crystals and Liquid Crystals **48**, 219 (1978).

[23] R. Forst, H. Boysen, F. Frey, H. Jagodzinski, and C. Zeyen, Journal of Physics and Chemistry of Solids **47**, 1089 (1986).

[24] R. Forst, H. Jagodzinski, H. Boysen, and F. Frey, Acta Crystallographica Section B **46**, 70 (1990).

[25] K. D. M. Harris and J. M. Thomas, J. Chem. Soc., Faraday Trans. **86**, 2985 (1990).

[26] R. Lynden-Bell, Molecular Physics **79**, 313 (1993).

[27] M. D. Hollingsworth and K. Harris, Urea, thiourea and selenourea inclusion compounds, in *Comprehensive Supramolecular Chemistry*, Vol. 6, edited by D. D. MacNicol (Elsevier Science, 1996) Chap. 7, pp. 177–237.

[28] T. Weber, H. Boysen, M. Honal, F. Frey, and R. B. Neder, Zeitschrift für Kristallographie - Crystalline Materials **211**, 238 (1996).

[29] R. Lefort, J. Etrillard, B. Toudic, F. Guillaume, T. Breczewski, and P. Bourges, Phys. Rev. Lett. **77**, 4027 (1996).

[30] T. Weber, H. Boysen, and F. Frey, Acta Crystallographica Section B **56**, 132 (2000).

[31] B. Toudic, P. Garcia, C. Odin, P. Rabiller, C. Ecolivet, E. Collet, P. Bourges, G. J. McIntyre, M. D. Hollingsworth, and T. Breczewski, Science **319**, 69 (2008).

[32] B. Toudic, F. Aubert, C. Ecolivet, P. Bourges, and T. Breczewski, Phys. Rev. Lett. **96**, 145503 (2006).

[33] Toudic, B., Rabiller, P., Bourgeois, L., Huard, M., Ecolivet, C., McIntyre, G. J., Bourges, P., Breczewski, T., and Janssen, T., EPL **93**, 16003 (2011).

[34] C. Mariette, M. Huard, P. Rabiller, S. M. Nichols, C. Ecolivet, T. Janssen, K. E. Alquist, M. D. Hollingsworth, and B. Toudic, The Journal of Chemical Physics **136**, 104507 (2012).

[35] C. Mariette, L. Guérin, P. Rabiller, C. Ecolivet, P. García-Orduña, P. Bourges, A. Bosak, D. de Sanctis, M. D. Hollingsworth, T. Janssen, and B. Toudic, Phys. Rev. B **87**, 104101

(2013).

[36] L. Guérin, C. Mariette, P. Rabiller, M. Huard, S. Ravy, P. Fertey, S. M. Nichols, B. Wang, S. C. B. Mannsfeld, T. Weber, M. D. Hollingsworth, and B. Toudic, Physical review. B, Condensed matter and materials physics **91** (2015).

[37] S. Zerdane, C. Mariette, G. J. McIntyre, M.-H. Lemée-Cailleau, P. Rabiller, L. Guérin, J. C. Ameline, and B. Toudic, Acta Crystallographica Section B **71**, 293 (2015).

[38] C. Mariette, I. Frantsuzov, B. Wang, L. Guérin, P. Rabiller, M. D. Hollingsworth, and B. Toudic, Physical Review B **94**, 184105 (2016).

[39] C. Ecolivet, M. Verezhak, C. Mariette, L. Guérin, P. Rabiller, J. Ollivier, A. Bosak, and B. Toudic, Phys. Rev. B **98**, 224308 (2018).

[40] T. Weber, Modulierte strukturen und Fehlordnung in Harnstoffeinschlussverbindungen bei Temperaturen von 30 bis 300 K, unpublished (1997).

[41] A. López-Echarri, I. Ruiz-Larrea, A. Fraile-Rodríguez, J. Díaz-Hernández, T. Breczewski, and E. H. Bocanegra, Journal of Physics: Condensed Matter **19**, 186221 (2007).

[42] M. Couzi, F. Guillaume, K. D. M. Harris, B. A. Palmer, K. Christensen, and S. P. Collins, EPL (Europhysics Letters) **116**, 56001 (2016).

[43] K. Christensen, P. A. Williams, R. Patterson, B. A. Palmer, M. Couzi, F. Guillaume, and K. D. M. Harris, Royal Society Open Science **6**, 190518 (2019).

[44] M. Couzi, F. Guillaume, and K. D. M. Harris, Royal Society Open Science **5**, 180058 (2018).

[45] B. Toudic, L. Guérin, C. Mariette, I. Frantsuzov, P. Rabiller, C. Ecolivet, T. Janssen, and M. D. Hollingsworth, EPL (Europhysics Letters) **119**, 66004 (2017).

[46] B. Toudic, L. Guérin, C. Mariette, I. Frantsuzov, P. Rabiller, C. Ecolivet, and M. D. Hollingsworth, Royal Society Open Science **6**, 182073 (2019).

[47] T. Weber, H. Boysen, F. Frey, and R. B. Neder, Acta Crystallographica Section B **53**, 544 (1997).

[48] B. Toudic, R. Lefort, C. Ecolivet, L. Guérin, R. Currat, P. Bourges, and T. Breczewski, Phys. Rev. Lett. **107**, 205502 (2011).

[49] H. T. Stokes, B. J. Campbell, and S. van Smaalen, Acta Crystallographica Section A **67**, 45 (2011).